Available online at www.sciencedirect.com
ScienceDirect
International Journal of Heat and Fluid Flow 28 (2007) 1167–1177
International Journal of HEAT AND FLUID FLOW
www.elsevier.com/locate/ijhff

Heat transfer and pressure drop characteristics of mini-fin structures

Pei-Xue Jiang *, Rui-Na Xu

Key Laboratory for Thermal Science and Power Engineering of Ministry of Educations, Department of Thermal Engineering, Tsinghua University, Beijing 100084, China

Received 16 March 2006; received in revised form 26 September 2006; accepted 7 November 2006
Available online 6 February 2007

Abstract

Forced convection heat transfer of air and water in bronze and pure copper mini-fin structures and mini-channel structures was investigated experimentally. The mini-fin dimensions were 0.7 mm × 0.2 mm and 0.8 mm × 0.4 mm. The tests included both staggered diamond-shaped and in-line square mini-fin arrangements. The tests investigated the effects of structures, mini-fin dimensions and arrangement, test section materials, and fluid properties on the convection heat transfer and heat transfer enhancement. For the tested conditions, the convection heat transfer coefficient was increased 9–21 fold for water and 12–38 fold for air in the mini-fin structures compared with an empty plate channel. The friction factor and flow resistance in the mini-channel structures and the in-line square mini-fin arrangement were much less than in the staggered diamond-shaped mini-fin arrangement. For the small channel width, $W_c = 0.2$ mm, the convection heat transfer with the in-line square array structure was more intense than with the staggered diamond-shaped structure, the mini-channel structure or the porous media. For the larger channel width, $W_c = 0.4$ mm, the convection heat transfer in the staggered diamond-shaped array structure was more intense than in the others systems while the in-line square structure had the best overall thermal-hydraulic performance.

Keywords: Mini-fin; Mini-channel; Experiment; Convection heat transfer

1. Introduction

Pin fins are cylinders or other shaped elements that are attached perpendicular to a wall. Various parameters characterize the pin fins, such as height, shape, diameter, and height to diameter ratio. Furthermore, pin fins may be positioned in either staggered or in-line arrangements with respect to the flow direction.

Sparrow and Ramsey (1978) and Sparrow and Kadle (1986) were among the first to investigate the heat transfer performance of in-line and staggered wall attached arrays of cylindrical fins, using fins 2.54 mm in diameter spaced 5.08 mm apart. Tanda (2001) analyzed the heat transfer and pressure drop in a rectangular channel equipped with arrays of diamond-shaped pin fins that were 5 mm wide with 20–40 mm between fins. The diamond-shaped elements were made of Plexiglas and, owing to their low thermal conductivity, the thermal boundary condition was considered to be adiabatic. Both in-line and staggered fin arrays were considered. Thermal performance comparisons with data for a rectangular channel without fins showed that the presence of diamond-shaped elements enhanced the heat transfer for equal mass flow rates and equal pumping power. Sara (2003) presented the heat transfer and friction characteristics and performance analysis of convective heat transfer through a rectangular channel with square cross-section pin fins attached to a flat surface. The pin fins were staggered and were 10 mm wide with 15–90 mm between fins. The experimental results showed that the square cross-section pin fins may provide better heat transfer enhancement. Bilen et al. (2001) did an experimental study on the heat transfer and friction loss characteristics of a surface with cylindrical fins in a rectangular cross-section channel with large diameter fins and different channel

* Corresponding author. Tel.: +86 10 62772661; fax: +86 10 62770209.
E-mail address: Jiangpx@mail.tsinghua.edu.cn (P.-X. Jiang).

0142-727X/$ - see front matter © 2006 Elsevier Inc. All rights reserved.
doi:10.1016/j.ijheatfluidflow.2006.11.008

Nomenclature

d_p	particle diameter, m
D_e	mini-fin and porous plate channel hydraulic diameter, m
f	$\Delta p/\frac{1}{2}\rho u^2\frac{L}{De}$, friction factor
h	average heat transfer coefficient, W/(m^2 K)
h_x	local heat transfer coefficient, W/(m^2 K)
j	$StPr^{2/3}$, Colburn factor
St	$Nu/RePr$, Stanton number
L	channel length, m
G	mass flow rate, kg/s
Nu	Nusselt number
Δp	pressure drop, Pa
Pr	Prandtl number
q	heat flux, W/m^2
Re	$\rho_f u_f D_e/\mu_f$, Reynolds number based on the plate channel hydraulic diameter
T	temperature, K
W_w	fin width, m
W_c	mini-channel width and distance between adjacent mini-fins, m
u_p	fluid velocity in the x direction, m/s
x, y	coordinates, m

Greek symbols

λ	thermal conductivity, W/(m K)
μ_f	fluid absolute viscosity, N s/m^2
ρ	fluid density, kg/m^3
ε	Porosity

Subscripts

e	effective
f	fluid
x	local
0	initial

geometries. The experiments were performed with in-line and staggered fin arrangements. The results indicated that the staggered array had a little better heat transfer enhancement than the in-line arrangement. The cylindrical fins were 17 mm in diameter and were spaced 30 mm apart, while the Reynolds number range was 3700–30 000.

In the past 20 years, convection heat transfer in microchannel structures has been studied extensively both numerically and experimentally to enhance the heat transfer. Guo and Li (2003) reviewed and discussed the size effects on microscale single-phase fluid flow and heat transfer. A detailed numerical simulation of forced convection heat transfer occurring in silicon-based microchannel heat sinks was conducted by Li et al. (2004) using a simplified three-dimensional conjugate heat transfer model (2D fluid flow and 3D heat transfer).

A porous media in the flow channel intensifies mixing of the fluid flow and increases the contact surface with the coolant, so porous structures are an effective heat transfer augmentation technique (Lage et al., 1996; Ould-Amer et al., 1998; Jiang et al., 1999, 2004a,b; Alkam et al., 2001; Tzeng et al., 2006; Hetsroni et al., 2006). The porosity variation next to the solid wall has been analyzed by many researchers (Benenati and Brosilow, 1962; Vortmeyer and Schuster, 1983; Vafai, 1984; Vafai et al., 1985; Cheng et al., 1991; Chen et al., 1996; Jiang et al., 1996; Moise and Tudose, 1998; Fu and Huang, 1999). This non-uniform porosity distribution leads to a maximum velocity within the high-porosity region, which is recognized as the flow-channeling phenomenon. Experiments have demonstrated that to improve the heat transfer, the porosity in the vicinity of the solid boundary should be reduced. The mini-fin structure can be conceptualized as a pin fin structure with very small dimensions as a kind of constant porosity porous structure (Jiang et al., 2004c).

The mini-fin, mini-channel and porous media structures are all effective heat transfer enhancement methods. Jiang et al. (2004c) studied the heat transfer and fluid flow of water and air in constant porosity mini-fin structures and in sintered porous media. The results showed that the friction factor and flow resistance in the mini-fin structure with higher porosity were much less than in the other mini-fin structures and in the sintered porous media. The heat transfer coefficients in the mini-fin structure were larger than in the sintered porous plate channel with the same porosity and material and similar dimensions. However, this previous research was preliminary and did not include the mini-channel data in Jiang et al. (2004c).

This paper presents extensive experimental data for staggered diamond-shaped mini-fins, in-line square mini-fins, sintered porous media and mini-channel structures. The mini-fin width and the distance between adjacent fins were both less than 0.8 mm. The flow resistances and heat transfer coefficients in the staggered diamond-shaped mini-fin structures, in-line square mini-fins, sintered porous media and mini-channel structures were compared to analyze the influence of structure, fin shape and fin arrangement on the flow resistance and convection heat transfer.

2. Experimental system and test sections

The physical model and the test section geometry are shown in Fig. 1. The test section dimensions were 39.6 mm × 39.6 mm × 4 mm with a heated section 38.6 mm × 35.8 mm × 4 mm. The channel upper surface received a constant heat flux, q_w, while the bottom and side plates were adiabatic. The flow entered the channel with an average velocity, u_o, and constant temperature, T_{f0}.

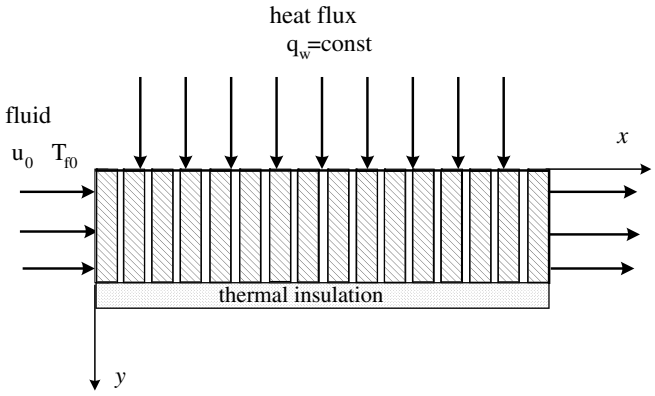

Fig. 1. Physical model and test section geometry.

The present study experimentally investigated the convection heat transfer in the mini-fin and mini-channel structures. The test sections were made from pure copper and bronze plates by wire machining. The channel height and the mini-fin height were both 4 mm. The test section upper plate was 1.0 mm thick. Jiang et al. (2004c) experimentally investigated forced convection heat transfer in mini-fin structures with staggered diamond-shaped fins. This study considers both in-line square mini-fins and mini-channel arrangements. The cross-sections of the staggered diamond-shaped mini-fins, the in-line square mini-fins and the mini-channel structures are shown in Fig. 2. The fin width, W_w, and the distance between adjacent fins, W_c, were varied in the different structures. The dimensions of all the test sections are listed in Table 1. Jiang et al. (2004c) already analyzed the experimental convection heat transfer results for test section Nos. 1, 2, 5, 6, 9 and 10. This work adds experimental data for test section Nos. 3, 4, 7 and 8 for comparison with the other test sections.

The experimental systems used to investigate the convection heat transfer of water and air in the mini-fin (or channel) structures and the experimental methods including the thin film heater, the sealing method, the temperature and mass flow rate measurements, and the data reduction method are all the same as those used in previous experimental research on forced convection heat transfer of water and air in mini-fin structures described by Jiang et al. (2004c). A detailed numerical analysis showed

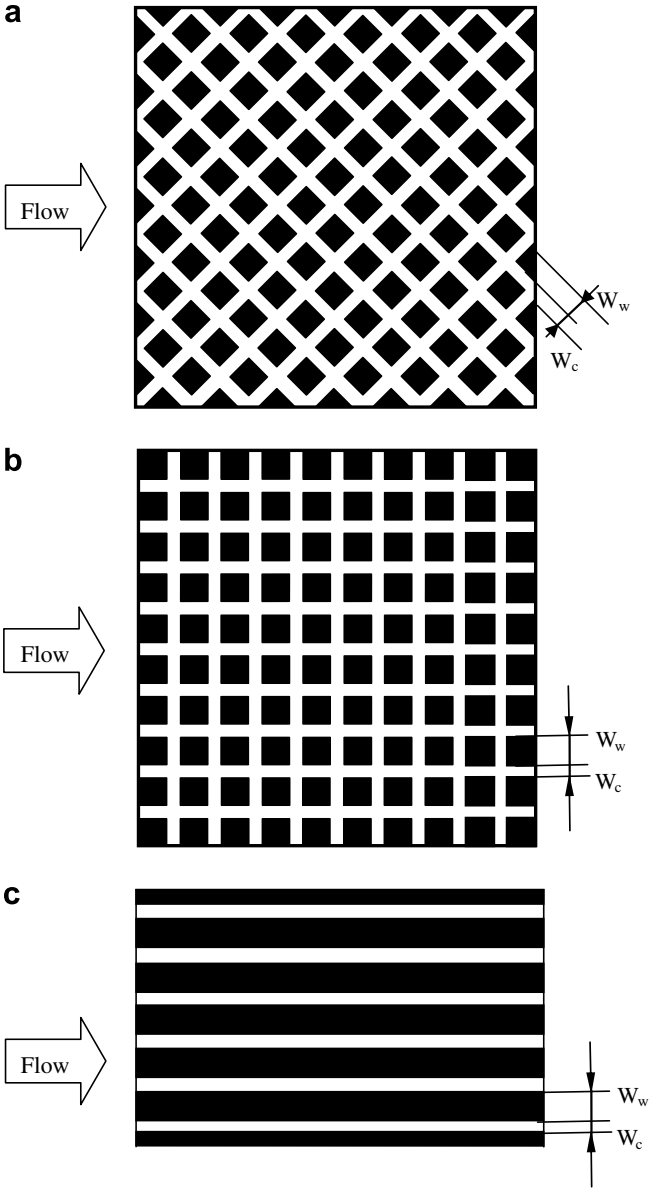

Fig. 2. Cross-section of the mini-fin structures (the black areas are the mini-fins which were made from pure copper and bronze by wire machining): (a) staggered diamond-shaped mini-fins, (b) in-line square mini-fin and (c) mini-channel.

that the heat transfer through the base plate is very close to one-dimensional so that the heat flux on the bottom sur-

Table 1
Test section dimensions

Test section	Fin geometry	Material	Structure	W_w	W_c	ε
No. 1	Diamond	Bronze	Mini-fin/staggered array	0.7	0.2	0.40
No. 2	Diamond	Copper	Mini-fin/staggered array	0.7	0.2	0.40
No. 3	Square	Bronze	Mini-fin/in-line array	0.7	0.2	0.40
No. 4	Channel	Bronze	Mini-channel	0.8	0.5	0.39
No. 5	Particle	Bronze	Sintered porous media	$d_p = 0.5$–0.71 mm		0.40
No. 6	Diamond	Copper	Mini-fin/staggered array	0.8	0.4	0.56
No. 7	Square	Copper	Mini-fin/in-line array	0.8	0.4	0.56
No. 8	Channel	Copper	Mini-channel	0.8	0.4	0.33
No. 9	Diamond	Copper	Mini-fin/staggered array	0.8	0.2	0.36
No. 10	Diamond	Copper	Mini-fin/staggered array	0.8	0.8	0.75

face of the test section was sufficiently uniform when using this heater.

Local temperatures along the plate channel were measured with eight copper–constantan thermocouples. The thermocouples were inserted into the upper plate of the test section (0.5 mm deep) along the centerline. The inlet fluid temperature was measured by two thermocouples in the inlet duct, approximately 6 cm upstream from the heated section. Three thermocouples were located at the outlet of the plate channel, approximately 6 cm downupstream from the heated section to measure the bulk temperature at the exit. Prior to installation, the thermocouples were calibrated using a constant-temperature oil bath. The overall accuracy was within ±0.1 °C. The inlet and outlet pressures were measured using accurate manometers with an accuracy of 0.25% of the full scale range of 0.1, 0.6 and 1.6 MPa. The mass flow rate for water was measured by weighting the fluid flowing from the channel for a given time period. The air volumetric flow rate was measured using two volumetric flow meters with accuracies of 1.4% of the full scale range of 7 N m^3/h and 45 N m^3/h. The experimental uncertainty for the heat balance was ±5%. The maximum errors in the flow rate were less than ±0.43% for water and ±2.4% for air.

The heat transfer coefficient and Nusselt number were defined as

$$h = \frac{q_w}{T_w - T_f}, \quad h_x = \frac{q_w}{T_{w,x} - T_{f,x}}, \quad Nu = \frac{h \cdot D_e}{\lambda}$$

where q_w is the wall heat flux, T_w is the average wall temperature of the plate surface adjacent to the fluid, T_f is the average fluid bulk temperature in the channel, $T_{w,x}$ is the local wall temperature of the plate surface adjacent to the fluid, and $T_{f,x}$ is the local cross-section average fluid temperature.

The experimental uncertainty in the convection heat transfer was mainly caused by experimental errors in the heat balance, axial thermal conduction in the plate test section, temperature measurement errors and the calculation of the surface temperature used for heat transfer coefficient. The experimental uncertainties in the convection heat transfer coefficient and pressure drop were estimated to be ±11.1% and ±3.0%.

3. Experimental results and discussion

Experimental measurements of the convection heat transfer in an empty plate channel were conducted before the experimental research on the convection heat transfer in the mini-fin and mini-channel structures to verify the test reliability. Jiang et al. (2004c) compared the experimental data with the calculated results for water and air flow in the empty plate channel. The standard deviation between the experimental results and predictions was ±10.0%. The accuracy of the experimental system is, therefore, deemed acceptable.

Mini-fin and mini-channel structures can be characterized as porosity porous media structures. Porosity is a very important parameter in porous media, so test section Nos. 1, 3–5 have the same porosity. Therefore, they were designed to estimate the effect of the different structures on the flow resistance and convection heat transfer. The fin width and the channel width are also very important factors in the design of fin structures. The mini-fin and mini-channel structures in test section Nos. 6–8 have the same fin width and the same channel width. Therefore, they were designed to estimate the effect of fin shape and arrangement on the flow resistance and convection heat transfer.

3.1. Flow resistance

3.1.1. Structure effect

Fig. 3 presents the friction factor, f, versus the Reynolds numbers for water and air in the mini-fin and mini-channel structure Nos. 1, 3 and 4. Although the porosities in the three sections are almost the same, the fin structures are different. The pressure drop in these structures increased and the friction factor decreased with increasing flow rate.

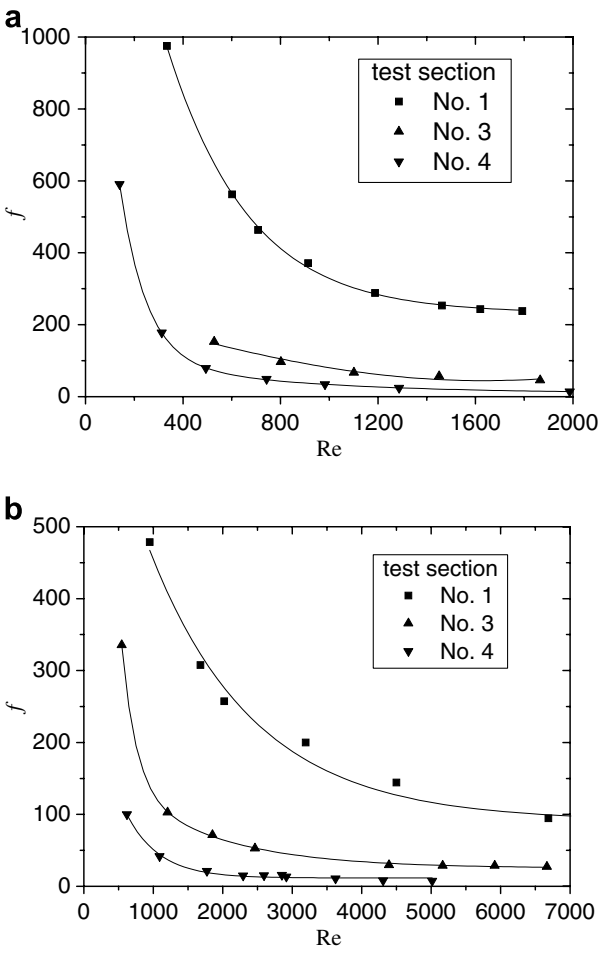

Fig. 3. Pressure drop for (a) water and (b) air in test section Nos. 1, 3 and 4.

The data in Fig. 3 shows that the friction factor in mini-channel structure No. 4 was much less due to the large channel width, W_c, and the simple channel structure. Comparing the friction factor in test section Nos. 1 and 3, the pressure drop in staggered array structure No. 1 was much larger than in the in-line array structure No. 3.

3.1.2. Fin shape and fin arrangement effect

Fig. 4 presents the friction factor versus the Reynolds numbers for water and air in the mini-fin and mini-channel structure Nos. 6–8. The channel width and the fin width of the three test sections are the same; however, the fin structures are different. Therefore, test section No. 8 has the lowest porosity. The friction factor in the staggered array structure No. 6 is much larger than in the in-line array structure No. 7. The same phenomenon is observed in Fig. 3. Generally, the staggered arrangement caused a larger flow resistance than the in-line arrangement with the mini-fins. This can be related to the complex fin arrangement. Fig. 4 shows that the friction factor for water flow in mini-channel No. 8 was more than that in mini-fin structure Nos. 6 and 7 at low velocities because the porosity in test section No. 8 was less than in the other two test sections. Comparing the friction factor in Figs. 3 and 4 shows that the flow resistance in the mini-fin structures with the larger porosity (e.g. 0.56) was much less than with the smaller porosity (e.g. 0.40).

3.2. Convection heat transfer

3.2.1. Local heat transfer coefficients

Fig. 5 presents the local heat transfer coefficient distributions for convection heat transfer of water and air in the plate channel with mini-fin structure No. 3. The local heat transfer coefficients for water in the mini-fin structures decreased significantly along the axial direction in the entry region, but the entry region effect for the heat transfer of air in the mini-fin structures was not significant. The local heat transfer coefficients increased near the outlet section due to axial heat conduction in the test section. The trends are similar in the other test sections in terms of the local heat transfer coefficient distributions for convection heat transfer of water and air. At all locations, the mini-fin structure greatly increased the heat transfer coefficients compared to the empty channel. For the studied conditions, the local heat transfer coefficients for water were enhanced 9–21 fold for test section Nos. 3, 4, 7 and 8. For air, the heat transfer coefficients were enhanced 12–38 fold for test sections Nos. 3, 4, 7 and 8 for the various

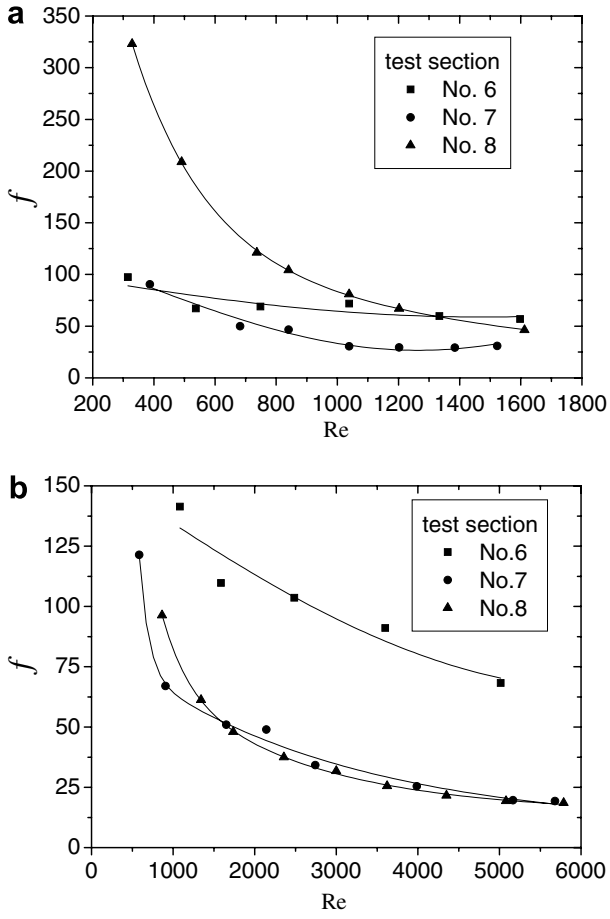

Fig. 4. Friction factor for (a) water and (b) air in test section Nos. 6–8.

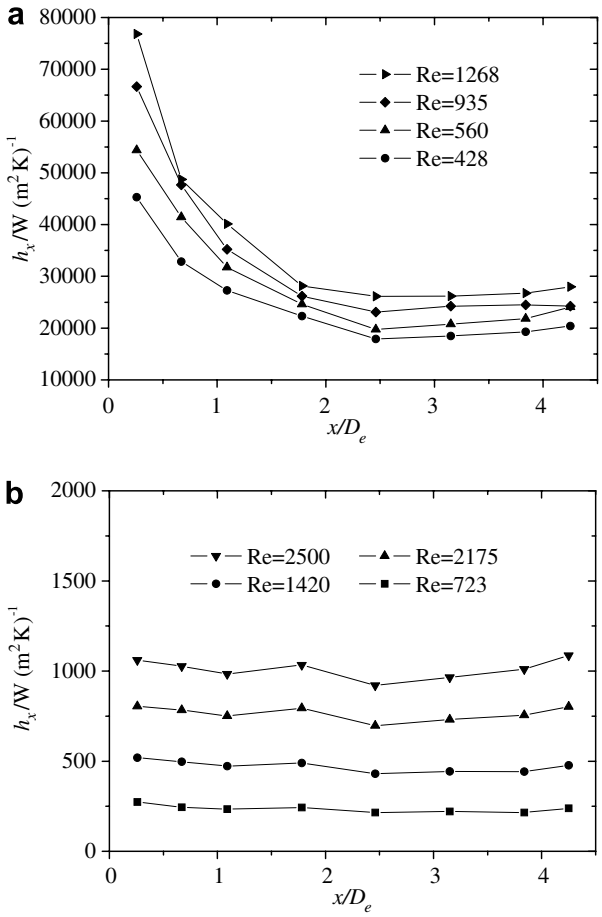

Fig. 5. Local heat transfer coefficients for (a) water and (b) air in mini-fin structure No. 3.

Table 2
Ratios of the heat transfer coefficients in the mini-fin structures with those in the empty channel

	No. 1	No. 2	No. 3	No. 4	No. 6	No. 7	No. 8	No. 9	No. 10
Water	10–16	18–21	13–17	9–12	21–24	19–21	13–15	13–14	14–16
Air	26–27	20–37	16–38	12–15	26–40	12–26	15–20	26–34	16–29

mass flow rates compared with the empty channel. Detailed comparisons for all test sections were listed in Table 2.

3.2.2. Structure effect

Fig. 6 compares the average Nusselt numbers in the test sections for convection heat transfer of water and air in the bronze mini-fin structures (Nos. 1 and 3) and the bronze mini-channel structure (No. 4) with those in the sintered bronze porous plate channel (No. 5) with a porosity of about 0.4. For the studied conditions with low flow rates, the heat transfer coefficients with the in-line square mini-fin arrangement, No. 3, were larger than with the other three sections for water. For low flow rates, the mixing effect caused by the staggered mini-fin array is not significant and the flow velocity in the staggered mini-fin array is lower due to the large number of flow channels compared with the in-line mini-fin array (see Fig. 2); therefore, the convection heat transfer in the staggered mini-fin array is less than in the in-line mini-fin array and in the parallel mini-channels. Fig. 6a shows that with increasing flow rate, the convection heat transfer in the staggered mini-fin channel increased more rapidly due to the intense mixing.

The heat transfer coefficients for air in the mini-fin structure Nos. 1 and 3 were quite similar. The heat transfer coefficients for water in mini-channel structure No. 4 were much higher than in the sintered bronze porous media, while the heat transfer coefficients for air in mini-channel structure No. 4 were the least of the four sections. For small Reynolds numbers, the larger heat transfer coefficients with water can be attributed to the good contact between the mini-channel and the upper plate, the larger

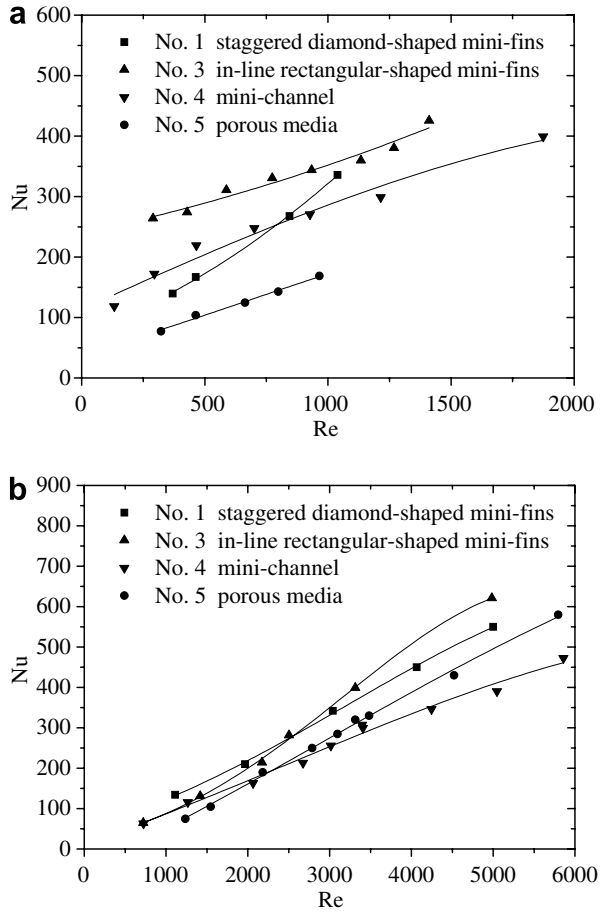

Fig. 6. Comparison of the average Nusselt number in the mini structure Nos. 1, 3–5: (a) water and (b) air.

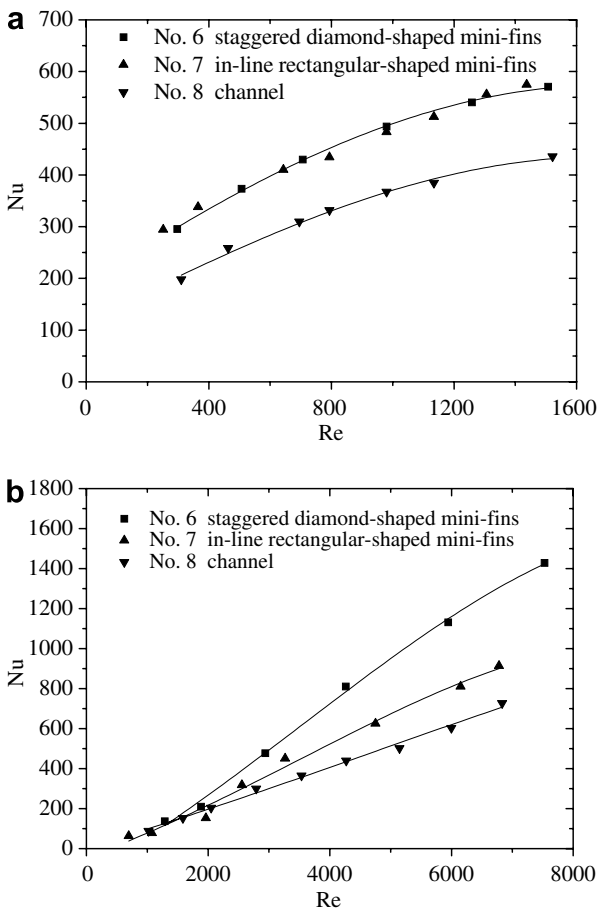

Fig. 7. Comparison of the average Nusselt numbers in mini structure Nos. 6–8: (a) water and (b) air.

effective thermal conductivity and the constant porosity in the mini-channel structure which differs from the plate channels filled with porous media, as shown by Jiang et al. (2004c). However, for large Reynolds numbers and for air flow, turbulent flow in the porous media enhances the convection heat transfer. In general, the heat transfer coefficients in mini-channel structure No. 4 were much lower at large Reynolds numbers than in the mini-fin structures with the same porosity. One reason is that for the same porosity the total heat transfer area of the mini-channel structure is much less than that of the mini-fin structures. Another reason is that the mini-channel structures do not enhance the mixing and turbulence.

3.2.3. Fin shape and fin arrangement effect

Fig. 7 compares the average Nusselt numbers for convection heat transfer of water and air in mini-fin structure Nos. 6 and 7 and in the mini-channel structure No. 8. The distance between adjacent fins and the mini-channel width, W_c, in test section Nos. 6–8 were all 0.4 mm. The staggered array more efficiently enhanced mixing and vortex creation than the in-line square array. For small Reynolds numbers, the total heat transfer area of test section Nos. 6 and 7 are similar and the mixing in the staggered array is not strong enough to significantly enhance the heat transfer. Therefore, the heat transfer coefficients for water in the staggered array structure No. 6 are similar to those in the in-line array structure No. 7. Nevertheless, the average Nusselt number for convection heat transfer of air in the staggered diamond-shaped mini-fins with high Reynolds number increased quickly with increasing Reynolds numbers. The rapid increase can be attributed to the greater mixing and vortex generation in the staggered array. The fluid flow in test section Nos. 6 and 7 was also numerically simulated with the details of the numerical results given in Appendix A. The convection heat transfer of water and air in the mini-channel structure No. 8 was much less than in the two mini-fin structure Nos. 6 and 7.

3.2.4. Material effect

Comparison of the Nusselt numbers in Figs. 6 and 7 shows that the convection heat transfer in the pure copper mini-fin structures with a larger porosity (e.g. 0.56) was much more intensive than in the bronze mini-fin structures with a lower porosity (e.g. 0.40). The same conclusion was drawn by Jiang et al. (2004c).

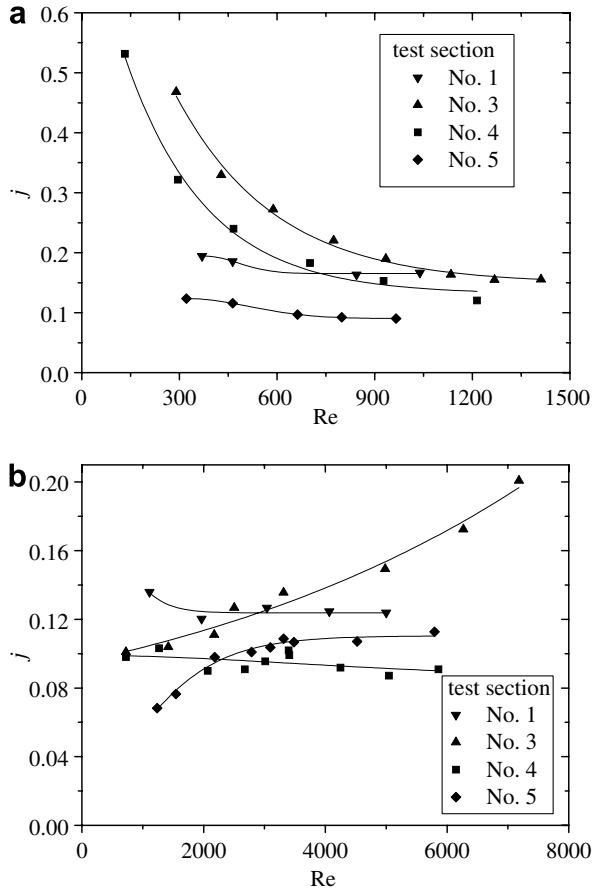

Fig. 8. j-Factors for (a) water and (b) air in mini structure Nos. 1, 3–5.

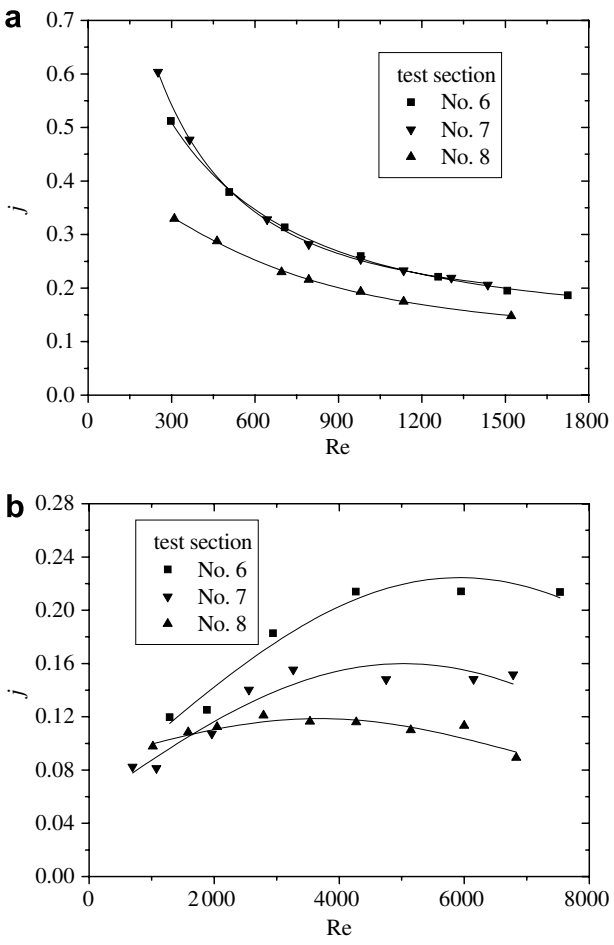

Fig. 9. j-Factors for (a) water and (b) air in mini structure Nos. 6–8.

3.2.5. Channel width effect

Figs. 8 and 9 compare the j-factor for convection heat transfer of water and air in the bronze test sections (Nos. 1, 3–5) and in the copper test sections (Nos. 6–8). The results show that for the small $W_c = 0.2$ mm, the convection heat transfer in the in-line square array structure was more intense than in the staggered diamond-shaped array structure, the mini-channel structure or the porous media. For the larger $W_c = 0.4$ mm, the convection heat transfer in the staggered diamond-shaped array structure was more intense than in the other structures. Therefore, for heat transfer enhancement, the staggered diamond-shaped array structure provides better enhancement at larger sizes and higher Reynolds numbers, while the in-line square array structure provides better enhancement for the smaller sizes.

3.3. Overall thermal-hydraulic performance

The ratios of the j-factor to the friction factor, f, in test section Nos. 1, 3–5 are presented in Fig. 10. For the same Reynolds number, the values of j/f for the in-line square-shaped mini-fin structure No. 3 and the mini-channel structure No. 4 are much larger than those in the staggered diamond-shaped array structure No. 1 or the sintered porous media with the mini-channel structure No. 4 having the largest values of j/f.

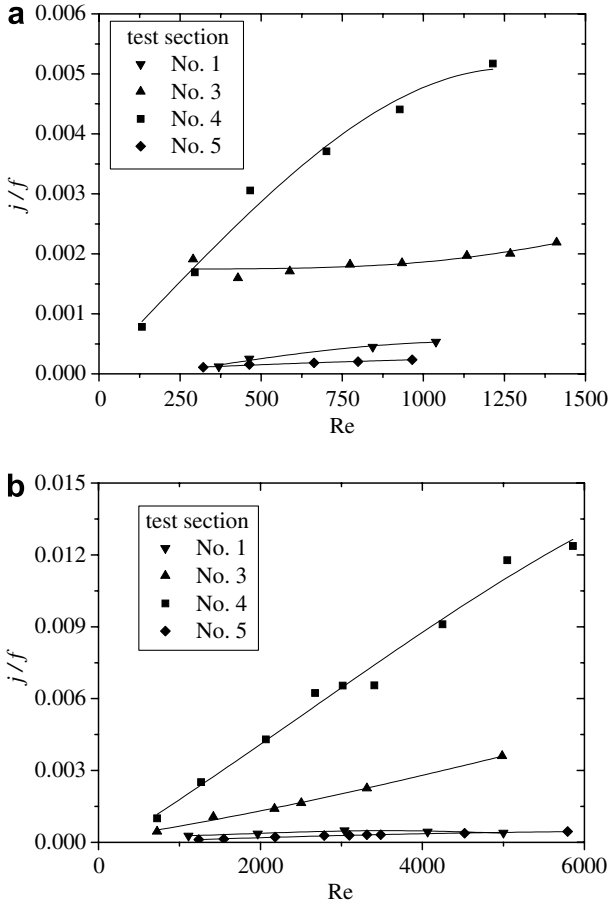

Fig. 10. Comparison of j/f for (a) water and (b) air in mini structure Nos. 1, 3–5.

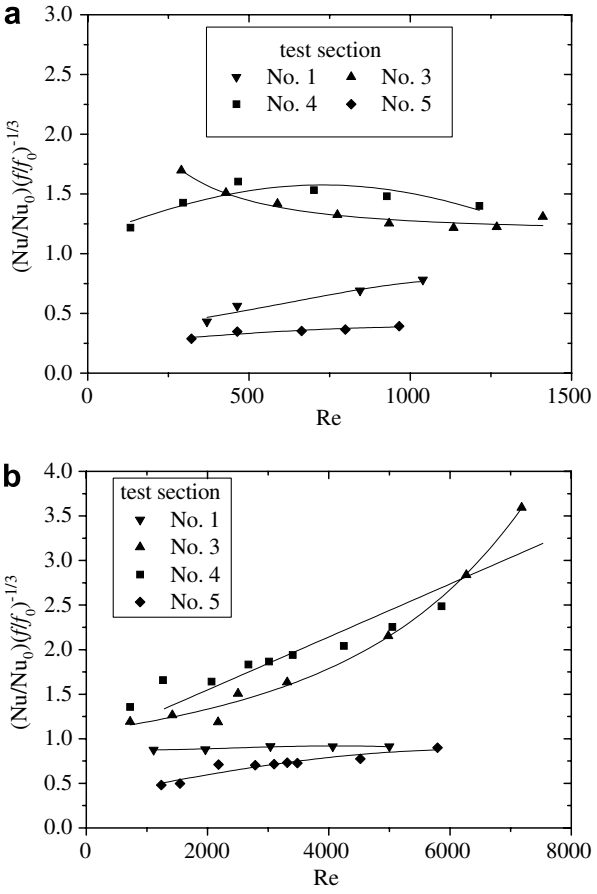

Fig. 11. Comparison of $(Nu/Nu_0)(f/f_0)^{-1/3}$ for (a) water and (b) air in test section Nos. 1, 3–5.

Fig. 11 presents the parameter $(Nu/Nu_0)/(f/f_0)^{1/3}$ for water and air in test section Nos. 1, 3–5. Nu_0 is the average Nusselt number for convection heat transfer in an empty plate channel and f_0 is the friction factor in an empty plate channel. Again, the mini-channel structure No. 4 and the in-line squared mini-fin structure No. 3 had the largest values of $(Nu/Nu_0)/(f/f_0)^{1/3}$. The sintered porous media had the lowest overall thermal-hydraulic performance. The values of $(Nu/Nu_0)/(f/f_0)^{1/3}$ for the in-line square fins and for the mini-channel structures were larger than one, which indicates that they are economical heat transfer enhancement structures. Generally, for the small mini-channel width, $W_c = 0.2$ mm, the mini-channel structure No. 4 had the best overall thermal-hydraulic performance with the in-line square structure also being an economical heat transfer enhancement structure.

Figs. 12 and 13 present the ratio of j to f and the parameter $(Nu/Nu_0)/(f/f_0)^{1/3}$ for water and air in test section Nos. 6–8 with $W_c = 0.4$ mm. The results show that for larger W_c, the in-line square fin structure No. 7 has the best overall thermal-hydraulic performance, while the mini-channel structure with the lower porosity, No. 8, has the lowest val-

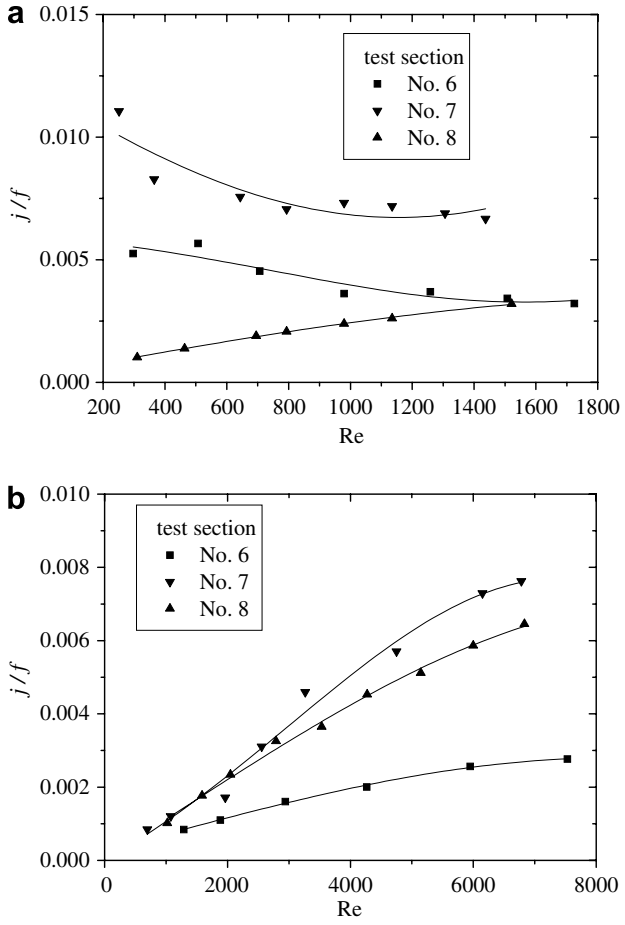

Fig. 12. Comparison of j/f for (a) water and (b) air in mini structure Nos. 6–8.

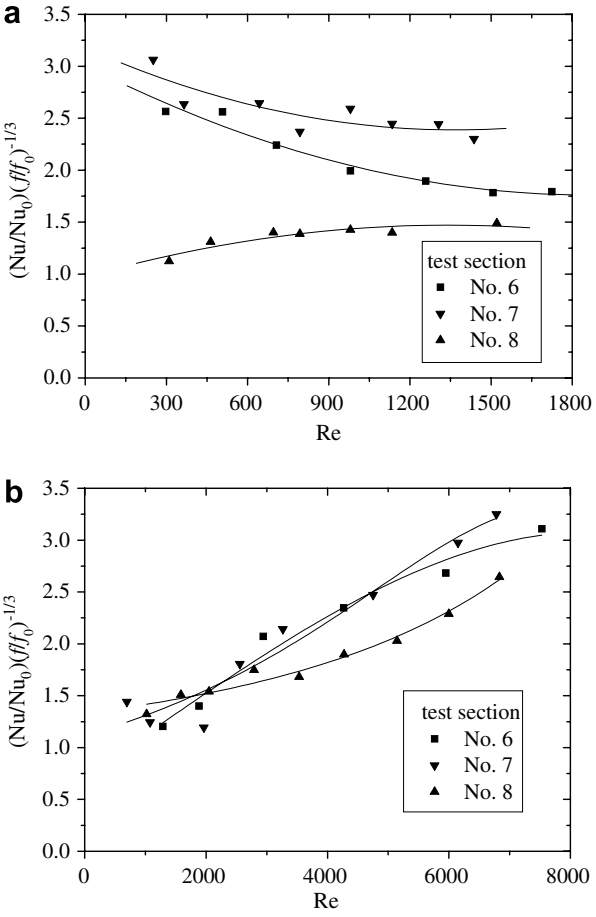

Fig. 13. Comparison of $(Nu/Nu_0)(f/f_0)^{-1/3}$ for (a) water and (b) air in test section Nos. 6–8.

ues of h/f and $(Nu/Nu_0)/(f/f_0)^{1/3}$. The values of $(Nu/Nu_0)/(f/f_0)^{1/3}$ in Fig. 13 for all three structures were all larger than one so they are all economical heat transfer enhancement structures.

Overall, the results show that the mini-fin structures have larger convection heat transfer coefficients and better overall thermal-hydraulic performance than the sintered porous media. The convection heat transfer coefficients and the overall thermal-hydraulic performance in the mini-fin structures and in the mini-channel structure depend on the channel width and shapes as well as the Reynolds number. Generally, for the small $W_c = 0.2$ mm, the convection heat transfer in the in-line square array structure No. 3 was more intense than in the staggered diamond-shaped structure No. 1, the mini-channel structure No. 4 or the porous media No. 5, while the mini-channel structure No. 4 and the in-line square array structure No. 3 had the best overall thermal-hydraulic performance. For larger $W_c = 0.4$ mm, the convection heat transfer in the staggered diamond-shaped array structure No. 6 was stronger than in the other structures due to the strong flow mixing, while the in-line square fin structure No. 7 had the best overall thermal-hydraulic performance.

4. Conclusions

(1) Comparison of structures with the same porosity shows that the flow resistance and heat transfer coefficients in the mini-channel structure are much lower than in the mini-fin structures with the same porosity.
(2) Comparison of fin structures with the same fin width and the same channel width, the flow resistance and convection heat transfer coefficients in the mini-fin structures with in-line arrays were much less than with the staggered array.
(3) For the smaller $W_c = 0.2$ mm, the convection heat transfer in the in-line square fin array structure No. 3 was more intense than in the staggered diamond-shaped structure No. 1, the mini-channel structure No. 4 or the porous media No. 5, while the mini-channel structure No. 4 and the in-line square fin array structure No. 3 had the best overall thermal-hydraulic performance.
(4) For the larger $W_c = 0.4$ mm, the convection heat transfer in the staggered diamond-shaped array structure No. 6 was stronger than in the other structures while the in-line square structure No. 7 had the best overall thermal-hydraulic performance.

Acknowledgements

The project was supported by the National Outstanding Youth Fund from the National Natural Science Foundation of China (No. 50025617), the Major State Basic Research Development Program (No. G1999033106) and the National Key Laboratory Fund (No. 51459030103JW0112).

Appendix A
Numerical simulation of fluid flow in test section Nos. 6 and 7

The flow characteristics of air in the staggered diamond-shaped (No. 6) and in-line square (No. 7) mini-fin arrangements was simulated numerically using a two-dimensional model in FLUENT 6.1. The Reynolds number was 6000, which is turbulent flow, so the RNG k–ε turbulence model was used with the enhanced wall functions. Further assumptions to simplify the model were that the flow was incompressible and the fluid properties were constant. Therefore, the governing equations were two-dimensional continuity, N-S equations and energy equation for incompressible turbulent flow. The boundary conditions at the fins were set as walls. The inflow into the domain was set as the mass flow inlet with the outflow set as the pressure outlet boundary condition. The other boundaries in the domain were all assumed to be symmetric. The equations were solved using the SIMPLEC velocity–pressure coupling and second order upwind discretization. The whole domain area was meshed with orthogonal rectangular elements, with 89,260 elements for the No. 6 geometry and 68,448 elements for the No. 7 geometry. The convergence criteria were 10^{-4} for continuity, momentum, k and ε. Converged results were attained after 2×10^4 iterations.

Fig. A.1 shows the numerically simulated velocity vectors and stream lines for air flow in the staggered array structure No. 6 and in the in-line array structure No. 7. The results show that for convection heat transfer of air at high Reynolds numbers, the staggered diamond-shaped mini-fins create enhanced mixing and vortex shedding which intensify the convection heat transfer and quickly increase the average Nusselt number with increasing Reynolds numbers. In the in-line square mini-fin structure, the air velocities between adjacent mini-fins perpendicular to the flow direction are quite low which is not beneficial for the convection heat transfer even though there are vortexes. Therefore, with increasing fluid velocity, the heat transfer in the staggered diamond-shaped mini-fin structure is expected to be much better than in the in-line square mini-fin structure.

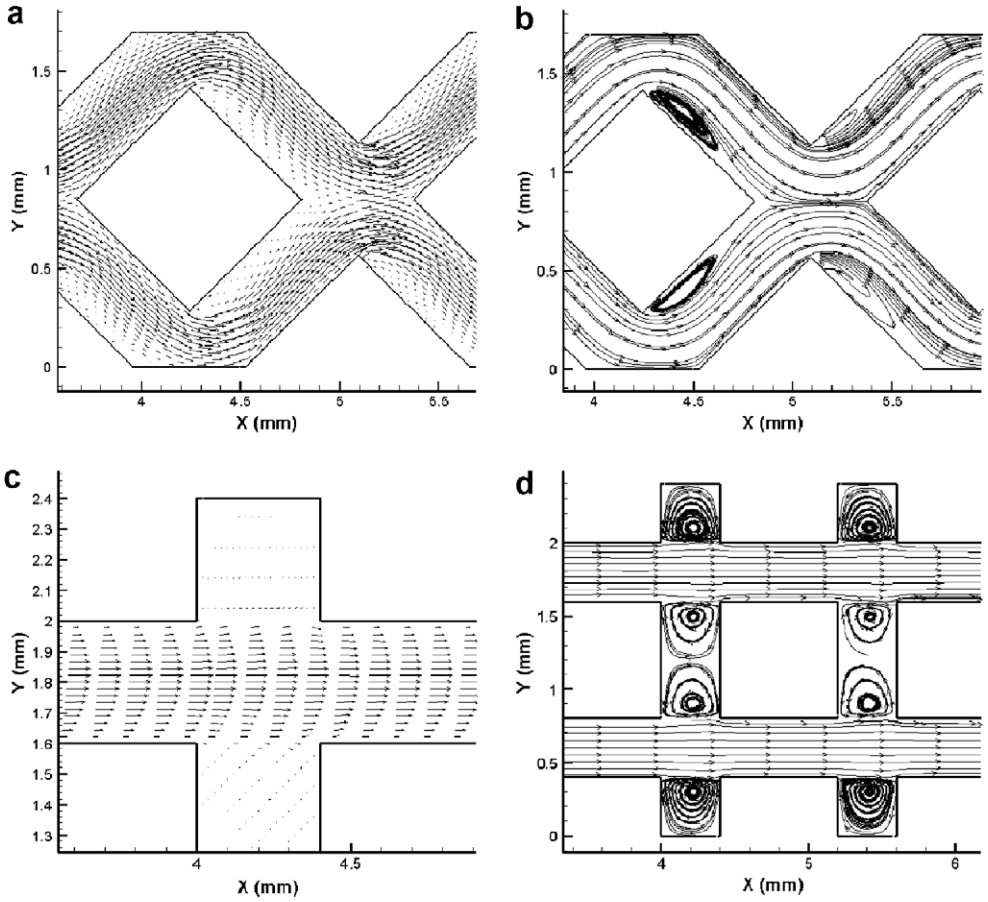

Fig. A.1. Velocity vectors and stream lines for air flow in the staggered array No. 6 and the in-line array No. 7 for $Re = 6000$.

References

Alkam, M.K., Al-Nimr, M.A., Hamdan, M.O., 2001. Enhancing heat transfer in parallel-plate channels by using porous inserts. International Journal of Heat and Mass Transfer 44, 931–938.

Benenati, R.F., Brosilow, C.B., 1962. Void fraction distribution in beds of spheres. AIChE Journal 8, 359–361.

Bilen, K., Akyol, U., Yapici, S., 2001. Heat transfer and friction correlations and thermal performance analysis for a finned surface. Energy Conversion and Management 42, 1071–1083.

Chen, C.H., Chen, T.S., Chen, C.K., 1996. Non-Darcy mixed convection along nonisothermal vertical surfaces in porous media. International Journal of Heat and Mass Transfer 39, 1157–1164.

Cheng, P., Chowdhury, A., Hsu, C.T., 1991. Forced convection in packed tubes and channels with variable porosity and thermal dispersion effects. Convective Heat and Mass Transfer in Porous Media, NATO ASI Series. Series E, Applied Sciences 196, 625–653.

Fu, W.S., Huang, H.C., 1999. Effects of a random porosity model on heat transfer performance of porous media. International Journal of Heat and Mass Transfer 42, 13–25.

Guo, Z.Y., Li, Z.X., 2003. Size effect on single-phase channel flow and heat transfer at microscale. International Journal of Heat and Fluid Flow 24, 284–298.

Hetsroni, G., Gurevich, M., Rozenblit, R., 2006. Sintered porous medium heat sink for cooling of high-power mini-devices. International Journal of Heat and Fluid Flow 27, 259–266.

Jiang, P.X., Wang, B.X., Luo, D.A., Ren, Z.P., 1996. Fluid flow and convective heat transfer in a vertical porous annulus. Numerical Heat Transfer, Part A 30, 305–312.

Jiang, P.X., Wang, Z., Ren, Z.P., Wang, B.X., 1999. Experimental research of fluid flow and convection heat transfer in porous plate channels filled with glass or metallic particles. Experimental Thermal and Fluid Science 20, 45–54.

Jiang, P.X., Li, M., Ma, Y.C., Ren, Z.P., 2004a. Boundary conditions and wall effect for forced convection heat transfer in sintered porous plate channels. International Journal of Heat and Mass Transfer 47, 2073–2083.

Jiang, P.X., Li, M., Lu, T.J., Yu, L., Ren, Z.P., 2004b. Experimental research on convection heat transfer in sintered porous plate channels. International Journal of Heat and Mass Transfer 47, 2085–2096.

Jiang, P.X., Xu, R.N., Li, M., 2004c. Experimental investigation of convection heat transfer in mini-fin structures and sintered porous media. Journal of Enhanced Heat Transfer 11, 391–405.

Lage, J.L., Weinert, A.K., Price, D.C., Weber, R.M., 1996. Numerical study of a low permeability microporous heat sink for cooling phased-array radar systems. International Journal of Heat and Mass Transfer 39, 3633–3647.

Li, J., Peterson, G.P., Cheng, P., 2004. Three-dimensional analysis of heat transfer in a micro-heat sink with single phase flow. International Journal of Heat and Mass Transfer 47, 4215–4231.

Moise, A., Tudose, R.Z., 1998. Air isothermal flow through packed beds. Experimental Thermal and Fluid Science 18, 134–141.

Ould-Amer, Y., Chikh, S., Bouhadef, K., Lauriat, G., 1998. Forced convection cooling enhancement by use of porous materials. International Journal of Heat and Fluid Flow 19, 251–258.

Sara, O.N., 2003. Performance analysis of rectangular ducts with staggered square pin fins. Energy Conversion and Management 44, 1787–1803.

Sparrow, E.M., Kadle, D.S., 1986. Effect of tip-to-shroud clearance on turbulent heat transfer from a shrouded, longitudinal fin array. ASME Journal of Heat Transfer 108, 519–524.

Sparrow, E.M., Ramsey, J.W., 1978. Heat transfer and pressure drop for a staggered wall-attached array of cylinders with tip clearance. International Journal of Heat and Mass Transfer 21, 1369–1377.

Tanda, G., 2001. Heat transfer and pressure drop in a rectangular channel with diamond-shaped elements. International Journal of Heat and Mass Transfer 44, 3529–3541.

Tzeng, S.C., Jeng, T.M., Wang, Y.C., 2006. Experimental study of forced convection in asymmetrically heated sintered porous channels with/without periodic baffles. International Journal of Heat and Mass Transfer 49, 78–88.

Vafai, K., 1984. Convective flow and heat transfer in variable-porosity media. Journal of Fluid Mechanics 147, 233–259.

Vafai, K., Alkire, R.L., Tien, C.L., 1985. An experimental investigation of heat transfer in variable porosity media. Journal of Heat Transfer 107, 642–649.

Vortmeyer, D., Schuster, J., 1983. Evaluation of steady flow profiles in rectangular and circular packed beds. Chemical Engineering Science 38, 1691–1699.